SECOND EUROPEAN CONFERENCE ON EARTHQUAKE ENGINEERING
AND SEISMOLOGY, ISTANBUL AUG. 25-29, 2014

SEISMIC ISOLATION: ASSESSMENT OF THE DAMPING CAPACITY

Todor ZHELYAZOV[1], Eythor Rafn THORHALLSSON[2], Simon ÓLAFSSON[3],
Jónas Thór SNÆBJÖRNSSON[4], and Ragnar SIGBJÖRNSSON[5]

ABSTRACT

The mechanical behaviour of lead-core bearing devices for seismic isolation is commonly described by a bi-linear or a Bouc-Wen hysteresis model. Using these models the parameters of the bearing device, such as damping capacity or energy dissipation capacity, can be evaluated.

In this article an accurate finite element model accounting for the material properties of the compounds of the seismic isolation device (steel, rubber, and lead-core material) is presented. After having defined the geometry and the mechanical characteristics of its compounds, the overall response of the bearing device can be obtained by simulating different excitation conditions.

The macro-behaviour can then be described in terms of the "displacement-shear force" relationship obtained by finite element analysis. Furthermore, based on this relationship, one of the commonly used macro models (e.g., bi-linear or Bouc-Wen hysteresis model) can be adjusted, and important parameters of the seismic isolation device, such as the damping capacity and the energy dissipation capacity, can be obtained.

INTRODUCTION

In this article some aspects of the mechanical behaviour of lead-core bearing devices for seismic isolation are considered. Commonly used mechanical models for the description of the global response of this type of seismic isolation devices are the bi-linear model and the Bouc-Wen hysteresis model (Bouc, 1967). The calibration of these models requires experimental data or, alternatively, reliable results obtained by finite element simulation. This article presents the result of an effort to employ the second option.

In order to define the mechanical parameters involved in the used material models, the bearing device should be subjected to different loading conditions (Aiken, 1992; Bessason, 1992). Thus, for example, in a typical characterization test, one of the surfaces of the bearing device is usually fixed, whereas on the opposite surface both constant vertical force (force parallel to the axis of the lead-core) and time-dependent horizontal force (force in a direction perpendicular to the axis of the lead-core) are applied. Furthermore, a set of data-points can be obtained by varying the magnitude of the sustained vertical load and the parameters of the time-dependent horizontal load (amplitude, frequency and magnitude of the applied force).

[1] Assist.Professor, Technical University, 8, St. Kl. Ohridski Blvd. Sofia, Bulgaria, todor.zhelyazov@tu-sofia.bg
[2] Assoc. Professor, Reykjavik University, Menntavegur 1, Reykjavik, Iceland, eythor@ru.is
[3] Research Professor, Earthquake Engineering Research Center, 800 Selfoss, Iceland, simon@hi.is
[4] Professor, Reykjavik University, Menntavegur 1, Reykjavik, Iceland, jonasthor@ru.is
[5] Professor, Earthquake Engineering Research Center, 800 Selfoss, Iceland, ragnar.sigbjornsson@hi.is

Roughly speaking, this phenomenological identification procedure could be replaced by tuning the mechanical model parameters, based on results obtained by finite element analysis. It should be clear that the finite element model itself should be phenomenological.

Assuming such an approach, which uses intensive finite element simulation, the experimental part of a time-consuming and costly characterization procedure can in general be significantly optimized.

A key issue in such studies is defining a rational way to evaluate the capacity of the seismic isolation device to modify the soil-superstructure interaction.

Hysteresis models allow the evaluation of parameters which quantify the capacity of seismic isolation devices to modify the seismic excitation while transferring it from the ground to the superstructure. Such parameters are, for instance, the damping capacity and the amount of the absorbed energy. These parameters can be evaluated, using common procedures after calibration of the model chosen to describe the overall mechanical behaviour of the seismic isolation device.

The authors are also interested in obtaining the mechanical response of the lead-core bearing device by performing a transient finite element analysis, using recorded strong-motion records as time-dependant excitation.

This article's plan is as follows: First the finite element model of the lead-core bearing device is presented. Details of the geometry, the boundary conditions and the employed finite elements are provided. The finite element model specification is followed by a discussion of the material models describing the mechanical behaviour of the seismic isolation device's compounds: rubber, steel, and lead applied for the lead-core. Furthermore, a finite element analysis procedure for simulating a typical characterization test is outlined. Some results obtained by finite element analysis are presented. Finally, a procedure is outlined for studying the mechanical behaviour of the seismic isolation device when it is subjected to real seismic excitation. The concluding remarks present the potential applications of the study reported and recommendations for further research.

FINITE ELEMENT MODEL

Figure 1 shows the geometry of the lead-core bearing device. The modelled cylindrical specimen (152mm in diameter) consists of 20 rubber layers, separated by 19 steel shims. Both rubber and steel layers are 3 mm in thickness. Steel plates, each 25 mm in thickness, are placed on the top and bottom sides of the specimen. The lead-core is a cylinder, 30 mm in diameter (Weisman and Warn, 2012).

An accurate finite element model in 3-D is created. Advantage is taken of the existing symmetries. Only half of the bearing device is modelled. Appropriate symmetry boundary conditions are defined on the plane of symmetry (see Figure 2).

All compounds of the bearing device are explicitly modelled. Volumes are created for the rubber layers and steel shims (see Figure 3), the lead-core and the thick top and bottom steel plates.

All the volumes are meshed using solid finite elements. The details of the finite elements employed are summarized in Table 1.

All the interfaces (the interface between the thick steel plate and the rubber layer, the interface between a rubber layer and a steel shim, the interface between the lead-core material and rubber and the interface between the lead-core and the steel) are assumed to give perfect bonds.

Explicit modelling enables accurate modelling and analysis of the interfaces between different materials.

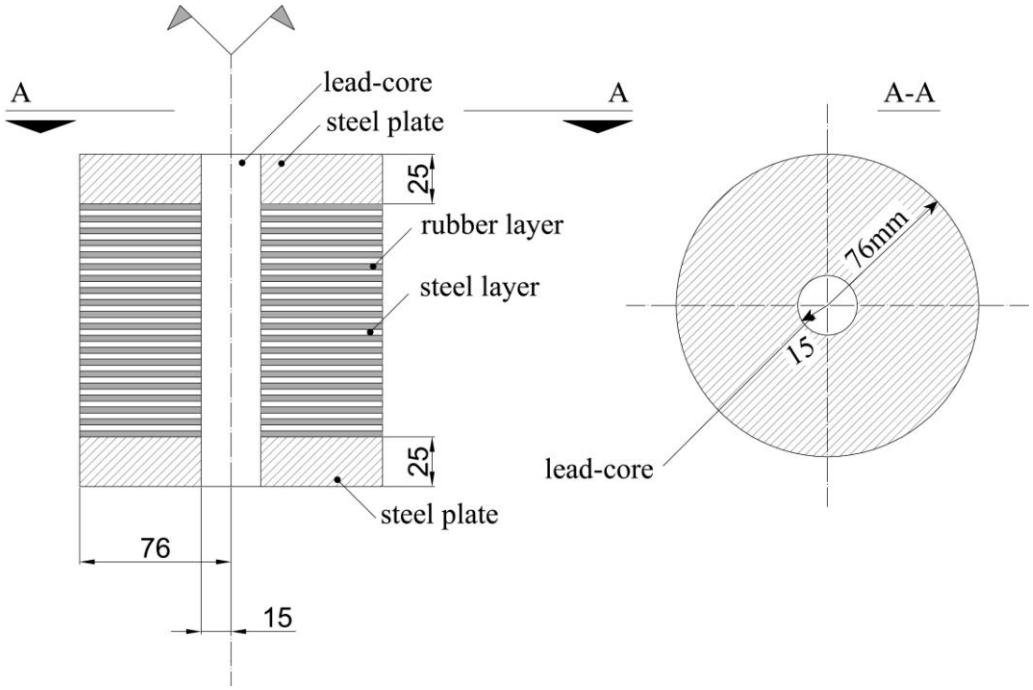

Figure 1. Geometry of the bearing device

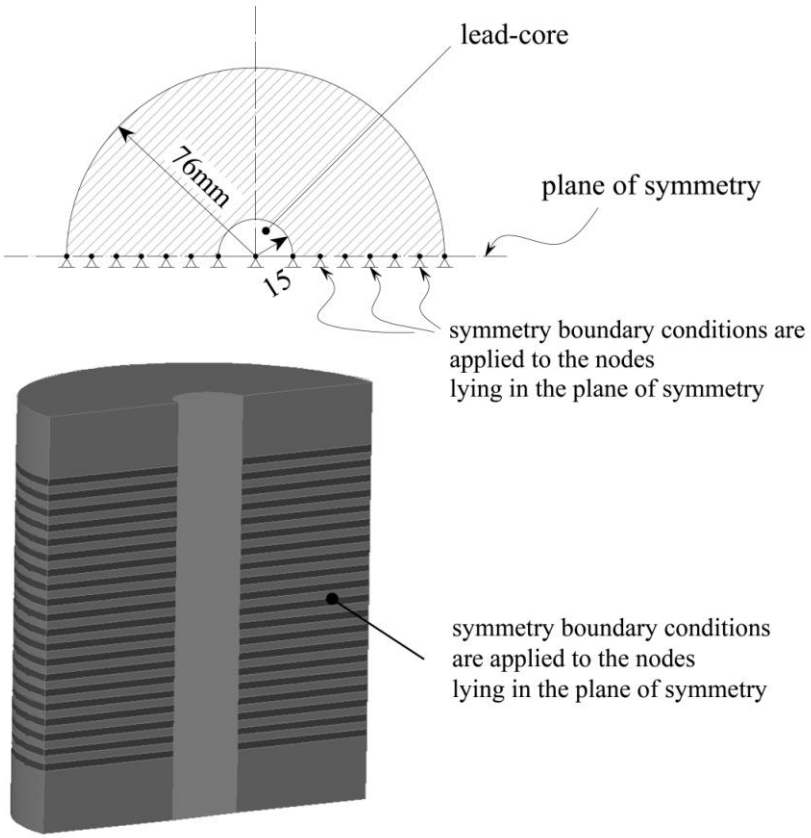

Figure 2. The half-space model and symmetry boundary conditions

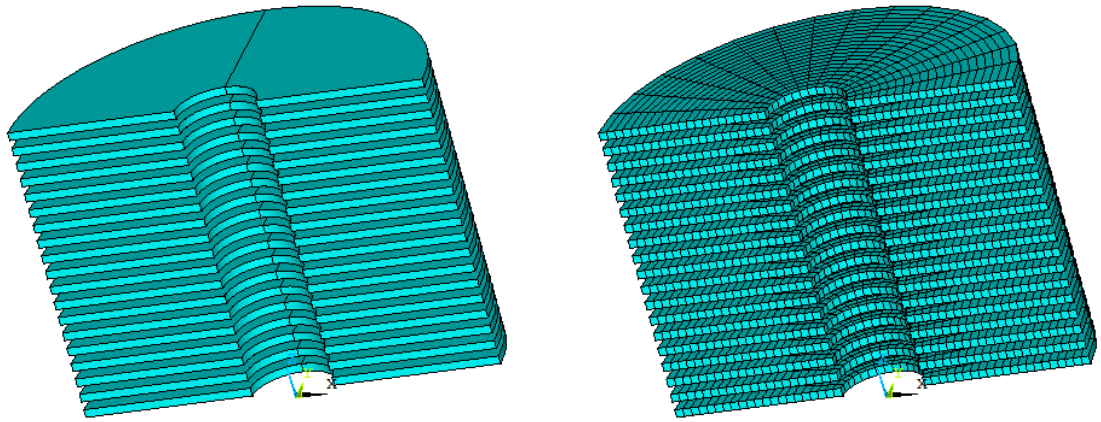

a) b)

Figure 3. Meshing of the steel layers: a) volumes created for the steel layers; b) generated mesh

Table 1. Finite elements specifications

Element type	Element description	Special capabilities	Used to mesh
Solid 95	20-node 3-D structural solid		✓ steel layers ✓ thick steel plates
Solid 185	20-node 3-D structural solid	simulating fully incompressible hyper-elastic materials	✓ lead-core ✓ rubber layers

MATERIAL MODELS

Material models are defined for the steel, the rubber and the lead-core material. The constitutive models of hyper-elastic materials are usually derived from strain energy potentials. Material models which are commonly used to simulate the mechanical behaviour of rubber are the neo-Hookean model and the Mooney-Rivelin model (Mooney, 1940).

NEO-HOOKEAN MODEL

For homogeneous isotropic materials the strain energy function can be expressed in terms of the stress invariants (Sino and Hughes, 1997). Thus, if a Neo-Hookean material model is chosen, the strain energy potential can be defined by the following equation:

$$W = \frac{\mu}{2}\left(\bar{I}_1 - 3\right) + \frac{1}{d}\left(J - 1\right)^2 \tag{1}$$

In Eq. (1) μ stands for the initial shear modulus of the material; d is the material incompressibility parameter, and $\bar{I}_1$ - is first stress invariant, i.e.:

$$I_1 = \lambda_1^2 + \lambda_2^2 + \lambda_3^2 \tag{2}$$

In Eq. (2) λ_1^2, λ_2^2 and λ_3^2 are the eigenvalues of the Cauchy-Green deformation tensor *C*. According to Ogden (1984) and Crisfield (1997), J can be seen as the ratio of the deformed elastic volume over the un-deformed reference volume of material. J can be evaluated in the following way:

$$J = \det\left[F_{ij}\right]. \tag{3}$$

In Eq. (3) F_{ij} denotes the components of the Lagrangian strain tensor. Furthermore, the modified invariants of *C* can be obtained as follows:

$$\bar{I}_k = I_k J^{-2/3}, k = 1,2,3 \tag{4}$$

The material incompressibility parameter d is related to the material bulk modulus K as follows:

$$K = \frac{2}{d} \tag{5}$$

and the Young's modulus of the material is defined as:

$$E = 2G(1+\nu) \tag{6}$$

MOONEY-RIVLIN MODEL

The strain-energy potential for the nine parameter Mooney-Rivlin model is defined by the following equation:

$$\begin{aligned} W &= C_{10}(\bar{I}_1 - 3) + C_{01}(\bar{I}_2 - 3) + C_{20}(\bar{I}_1 - 3)^2 + \\ &+ C_{11}(\bar{I}_1 - 3)(\bar{I}_2 - 3) + C_{02}(\bar{I}_2 - 3)^2 + C_{30}(\bar{I}_1 - 3)^2 + \\ &+ C_{21}(\bar{I}_1 - 3)^2(\bar{I}_2 - 3) + C_{12}2(\bar{I}_1 - 3)(\bar{I}_2 - 3)^2 + C_{03}(\bar{I}_2 - 3)^2 + \frac{1}{d}(J-1)^2 \end{aligned}. \tag{7}$$

The initial shear modulus is given by the following equation:

$$\mu = 2(C_{10} + C_{01}) \tag{8}$$

The bulk modulus can be obtained by using Eq. (5). In Eq. (7) and Eq. (8) C_{ij} are material model parameters which have to be experimentally defined. For the full cubic Mooney-Rivilin model nine constants have to be identified. It should be noted that a reduced two-constant Mooney-Rivelin model usually provides good results for rubber materials for strains up to 200%. It should be also noted that the Mooney-Rivlin model is just a polynomial approximation of the energy density (Milani and Milani, 2012).

For the finite element simulation reported in this article, the Neo-Hookean model is retained. Based on experimental data, the following values are chosen for the material parameters μ and d :

- ✓ μ = 0.73MPa; the result is obtained from a bearing characterization test (Weisman and Warn, 2012).
- ✓ d = 0.001 mm^2/N, which involves the assumption that the bulk modulus *K* of the rubber has the typical value of 2000 MPa (Weisman and Warn, 2012).

MATERIAL MODEL FOR STEEL

The behaviour of steel (thick steel plates and reinforcing steel shims between the rubber layers) is assumed to be isotropic, linear and homogeneous (Weisman and Warn, 2012). The mechanical response of steel can thus be obtained by defining Young's modulus, E_s and Poisson's ratio, υ_s. The values applied are: E_s = 200,000 MPa and υ_s= 0.3.

MATERIAL MODEL FOR THE LEAD-CORE

The mechanical response of the lead-core is simulated by postulating an elastic-plastic material model (Weisman and Warn, 2012; Warn and Whittaker, 2006). The response of the lead-core material in the plastic domain is modelled by introducing an isotropic hardening rule. It is also assumed that the material obeys the von Mises yield criterion.

The shear yield stress of the lead-core σ_L is taken to be equal to τ_y, where τ_y is commonly obtained as follows:

$$\tau_y = \frac{f_{y,lc}}{\sqrt{3}} \tag{9}$$

where $f_{y,lc}$ is the uniaxial yield strength of the lead-core. The following values are applied: $f_{y,lc}$ = 14.4 MPa and σ_L=8.3 MPa.

For the elasticity modulus, E_{lc}, and for Poisson's ratio, υ_{lc}, of the lead-core, the following values are retained (Guruswamy, 2000): E_{lc} = 16000 MPa and υ_{lc} = 0.44.

CHARACTERIZATION TEST: FINITE ELEMENT SIMULATION

A typical uniaxial characterization test is simulated by using the general purpose finite element software ANSYS (ANSYS Inc. Documentation for Release 14.5). The response of the lead-core bearing device is obtained by performing an explicit dynamic transient analysis. The equation of motion has the form:

$$[M]\{\ddot{u}\} + [D]\{\dot{u}\} + [K]\{u\} = \{F(t)\} \tag{10}$$

In Eq. (10) [M] is the mass matrix; [D] is the damping matrix; [K] is the stiffness matrix; $\{\ddot{u}\}$ is the nodal acceleration vector; $\{\dot{u}\}$ is the nodal velocity vector, and $\{u\}$ is the nodal displacement vector.

All the nodes on the 'bottom' surface of the bearing device (Z = -25mm) are restrained against all possible displacement (nodal translations along X-, Y- and Z-axis).

Both constant vertical loads and time-dependant horizontal loads are applied to the nodes on the 'top' surface of the bearing device (Z = 142mm). The vertical load is applied along the direction parallel to the global Z-axis in the model space. The time-dependant horizontal load is simulated by applying displacements to the top-surface-nodes in a direction parallel to the global X-axis. The pattern of the time-dependent horizontal load is summarized in Table 2.

The boundary conditions defined for the simulation of the characterization test are shown in Figure 4. In order to obtain the 'force-displacement' relationship, the evolution of the shear stresses along the global X-direction is monitored. For the monitoring of the shear stress, finite elements from the mesh generated in the lead-core volumes are chosen. The shear stress is monitored in the finite elements adjacent to the fixed surface of the lead-core seismic isolation device. Furthermore, the shear stresses are averaged, and the shear force is calculated for each load step by multiplying the averaged shear stress by the cross-sectional area of the lead-core.

Table 2. Time-dependant load for the characterization test

Load step No.	Time value at the end of the load step	Applied displacement (ramped)	Maximum number of sub-steps
1	20	0→30mm	50
2	40	30mm→0	50
3	60	0→-30mm	50
4	80	-30mm→0	50
5	100	0→30mm	50
6	120	30mm→0	50
7	140	0→-30mm	50
8	160	-30mm→0	50

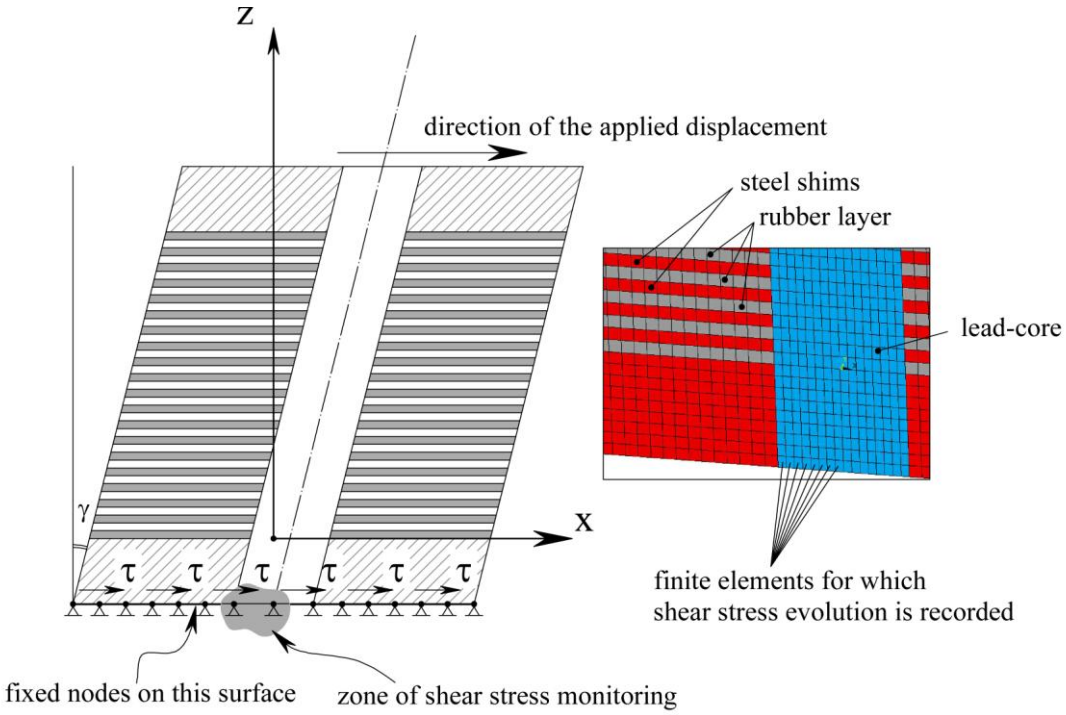

Figure 4. Schematization of the characterization test simulation

CHARACTERIZATION TEST: FINITE ELEMENT ANALYSIS RESULTS

Results obtained from the stress monitoring for all finite elements along the chosen path are shown in Figure 5. For the chosen meshing parameters there are eight finite elements along the chosen path (Figure 4). The shear stresses for each of the eight finite elements are obtained for each load step. Their evolution is plotted against time. Time appears as a tracking parameter in the transient analysis for each load step; both the magnitude of the applied load and the time are defined. The shear stress evolution displayed in Figure 5 is obtained for the load pattern given in Table 3.

Table 3: Time-dependant load for the characterization test

Load step No.	Time value at the end of the load step	Applied displacement (ramped)	Maximum number of sub-steps
1	7	0→5mm	150
2	14	5mm→10mm	150

Figure 5 is provided only to illustrate the scatter in the shear stress along the chosen path. It can be seen that the two load steps given in Table 3 are merely part of the first load step defined in Table 2.

After averaging the stresses and the calculation of the shear force, the latter is evaluated for each load step. The shear force is plotted for each load step against the applied displacements in Figure 6, where the hysteresis relationship of the action vs. displacement obtained by finite element analysis can be clearly seen.

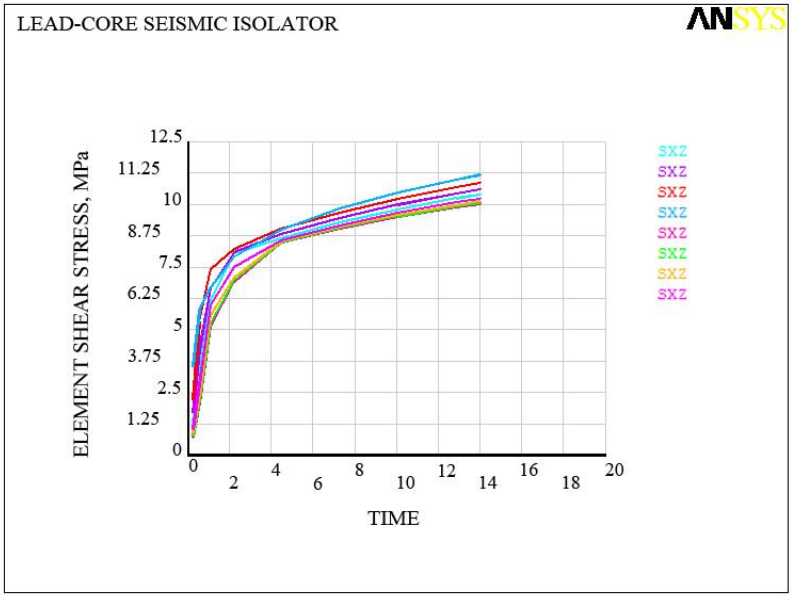

Figure 5. Evolution of the shear stresses in the monitored finite elements

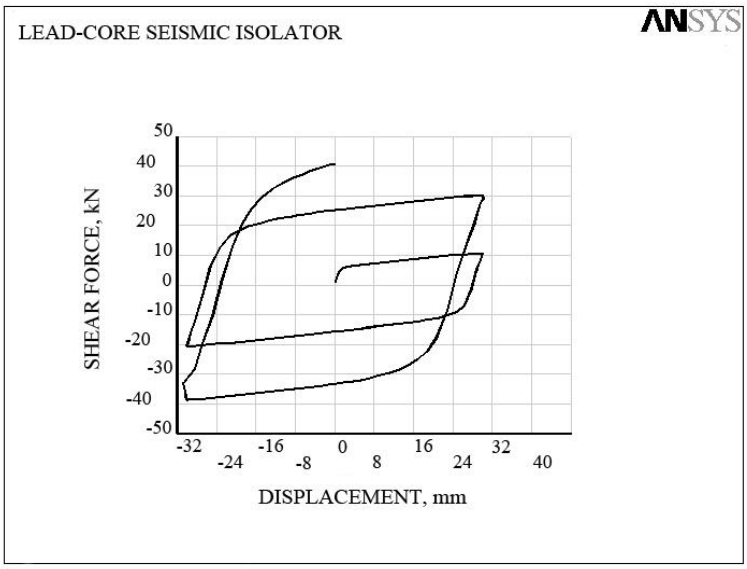

Figure 6. Shear force vs. displacements curve obtained by finite element simulation

SIMULATION OF THE BEARING DEVICE RESPONSE TO STRONG-MOTION RECORDS

In this section some basics of the procedure used to determine the mechanical response of the seismic isolation bearing device to recorded strong-motion are reported.

Records from near-fault strong-motion, obtained in earthquakes in Iceland (Sigbjörnsson et al., 2007), are employed. The recorded time series are supplied as data tables containing the X-, Y- and Z-components of the acceleration vector. The recorded time-series are read into the ANSYS software, where the input-arrays are dimensioned to fit the length of the time series.

In order to reduce the computational time, the sampling rate of the original arrays is reduced through decimation. The sampling frequency is reduced from 200 Hz to 50 Hz. The number of data points and, respectively, the number of load cases is also considerably reduced. A sample of the decimated time series for the X-component of the acceleration vector is plotted in Figure 7.

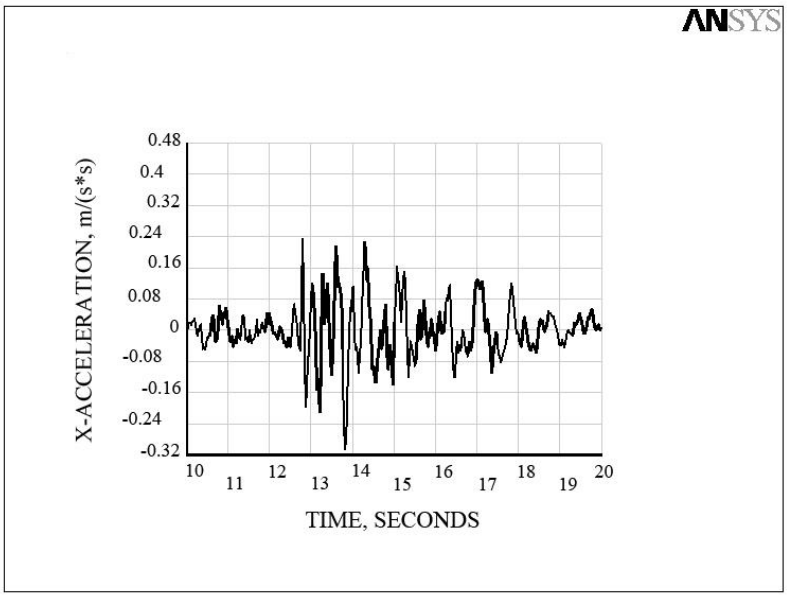

Figure 7. X-component of the acceleration input vector

Based on the acceleration time-series data stored, a time-dependent load is defined. For each data point a value of the displacement is obtained through integration with respect to time, using an average acceleration integration scheme where the magnitude of the acceleration within a time step (the time between two sampling values) is assumed constant. The necessary integration constants are tuned as follows: for the first step zero initial conditions are assumed, i.e., zero initial velocity and zero initial displacement; for each subsequent data point the values of the initial velocity and displacement are set equal to the velocity and displacement obtained through integration in the previous step.

The same procedure is performed to obtain the Y- and Z-components of the displacement vector.

The time-dependent action is applied to the nodes of the top surface of the bearing device, whereas the nodes on the bottom surface remain fixed. The action vs. displacement curve is obtained by monitoring the evolution of the shear stress in finite elements of the mesh generated in the lead-core.

CONCLUSIONS AND FURTHER RESEARCH

A numerical procedure has been created using the ANSYS Parametric Design Language (APDL). The procedure can be used for the parametric study of the mechanical response of lead-core rubber bearings for passive seismic isolation.

Based on the obtained action vs. displacement relationship one of the classical hysteresis model (equivalent bi-linear or Bouc-Wen hysteresis model) can be calibrated. Further the damping capacity and the amount of absorbed energy can be evaluated.

A possible alternative to the analytical models calibration is the definition of a super element which can be subsequently used in the super-structure modelling and in the analysis of the super-structure behaviour to seismic action.

It should be noted that all the necessary data for the finite element model formulation was taken from sources found in literature. In the next stage of this study, identification tests of the materials and a characterization test of the lead-core seismic isolation device should be performed to provide the phenomenological data needed for the constitutive laws calibration.

ACKNOWLEDGEMENT

The financial support to the first author by the Bulgarian Ministry of Education, Youth and Science for the realization of this study (project BG051PO001-3.3.05-0001) is gratefully acknowledged.

REFERENCES

Aiken ID, Kelly JM, Clark PW, Tamura K, Kikuchi M and Itoh T, (1992), "Experimental studies of mechanical characteristics of three types of seismic isolation bearings," *Proceedings, Tenth World Conference on Earthquake Engineering, Madrid*, Vol. 4,2281-2286

ANSYS Inc. Documentation for Release 14.5

Bessason B (1992) Assessment of earthquake loading and response of seismically isolated Bridges, Ph. D dissertation, Norwegian Institute of Technology.

Bouc R (1967) "Forced Vibration of Mechanical system with hysteresis", *Abstract, Proceedings of the 4th Conference on Nonlinear Oscillations*, Prague, Czechoslovakia

Crisfield MA (1997) Non-linear Finite Element Analysis of Solids and Structures, Vol. 2, Advanced Topics, John Wiley & Sons.

Guruswamy S (2000) Engineering properties and applications of lead alloys, Marcel Dekker, New York.

Milani G and Milani F (2012) Stretch-Stress Behavior of Elastomeric Seismic Isolators with Different Rubber Materials: Numerical insight. *Journal of Engineering Mechanics*, 138, 416-429.

Mooney M (1940) "A theory of large elastic deformation." *J. Appl. Phys.*, 11(9), 582–592.

Ogden RW (1984) Nonlinear Elastic Deformations, Dover Publications, Inc.

Sigbjörnsson R, Ólafsson S, & Snæbjörnsson JTh (2007) Macroseismic effects related to strong ground motion: a study of the South Iceland earthquakes in June 2000. *Bulletin of Earthquake Engineering*, *5*(4), 591-608.

Sigbjörnsson, R, Snæbjörnsson, JTh, Higgins, SM, Halldórsson, B, Ólafsson, S, (2009) A note on the Mw 6.3 earthquake in Iceland on 29 May. *Bulletin of Earthquake Engineering*, 113-126.

Simo JC and Hughes TJR (1997) *Computational Inelasticity*, Springer-Verlag.

Warn GP and Whittaker AS (2006) *A study of the coupled horizontal-vertical behavior of elastomeric and lead-rubber seismic isolation bearings*. MCEER-06-0011, Multidisciplinary Center for Earthquake Engineering Research, Buffalo, New York.

Weisman J and Warn GP (2012) Stability of Elastomeric and Lead-Rubber Seismic Isolation Bearings, *Journal of Structural Engineering*, 138(2):215-233.